

**Insight into neutrino mass phenomenology**  
**by exploring the non-relativistic regime in quantum field theory**

Apriadi Salim Adam,<sup>1,\*</sup> Nicholas J. Benoit,<sup>2,†</sup> Yuta Kawamura,<sup>2,‡</sup> Yamato  
Matsuo,<sup>2,§</sup> Takuya Morozumi,<sup>3,4,¶</sup> Yusuke Shimizu,<sup>3,4,\*\*</sup> and Naoya Toyota<sup>2,††</sup>

<sup>1</sup>*Research Center for Physics, Indonesian Institute of Sciences (LIPI),  
Serpong PUSPIPTEK Area, Tangerang Selatan 15314, Indonesia*

<sup>2</sup>*Graduate School of Science, Hiroshima University,  
Higashi-Hiroshima 739-8526, Japan*

<sup>3</sup>*Physics Program, Graduate School of Advanced Science and Engineering,  
Hiroshima University, Higashi-Hiroshima 739-8526, Japan*

<sup>4</sup>*Core of Research for the Energetic Universe, Hiroshima University,  
Higashi-Hiroshima 739-8526, Japan*

(Dated: June 8, 2021)

## Abstract

We present a novel formulation, based on quantum field theory, for neutrino oscillation phenomenology that can be applied to non-relativistic and relativistic energies for neutrinos. The formulation is constructed as a time evolution of a lepton family number operator. At time  $t = 0$ , we assign either a Dirac or Majorana mass to the neutrino. Then, the time evolution of the lepton family number operator becomes dependent on the mass and new features appear. We show in the non-relativistic regime, by taking the expectation value of the lepton number operator, the absolute mass hierarchy and the type of neutrino mass are distinguishable.

## INTRODUCTION

Neutrinos were originally formulated, within the weak interactions of the Standard Model (SM), to be massless fermions. However, hints of massive neutrinos appeared in the second half of the 20th century with the solar neutrino problem[1]. Eventually, updated solar models and experiments from the Kamiokande laboratory and the Sudbury Neutrino Observatory (SNO) proved the disappearance is caused by flavor oscillations[2, 3]. For neutrinos the existence of flavor oscillations mean there is a mixing between mass and flavor eigenstates. The mixing between mass and flavor is governed by the unitary PMNS matrix, which has six (four) free parameters in the  $3 \times 3$  case[4, 5]. Thus, the mixing caused by flavor oscillations is direct evidence that neutrinos are massive and, consequently, require physics beyond the SM.

In this decade, the six (four) parameters related to the PMNS matrix; the oscillation angles  $\theta_{12}, \theta_{23}$ , and  $\theta_{13}$ , the mass squared differences  $\Delta m_{21}^2$  and  $\Delta m_{31}^2$ , and the Dirac CP violating phase  $\delta_{cp}$ , are expected to be measured within a few percentages by neutrino oscillation experiments[6–11]. In addition, the absolute mass of the lightest neutrino,  $m_1$  or  $m_3$ , is expected to be directly limited down to the sub-eV range by the Karlsruhe Tritium Neutrino Experiment (KATRIN)[12]. However, even with these precision measurements, questions remain in neutrino phenomenology. Specifically, the question of what is the absolute mass hierarchy for neutrinos, normal  $m_1 < m_2 \ll m_3$  or inverted  $m_3 \ll m_1 < m_2$ , and the question of what type of mass neutrinos possess, Dirac or Majorana. Those questions could be answered by future neutrinoless double- $\beta$  ( $0\nu\beta\beta$ ) decay experiments[13–17]. Arguably, additional approaches to answer those questions would be ideal.

For this Letter, we present an unified description of neutrino phenomenology that leads to an additional approach for investigations of the previously mentioned questions. We define unified to mean a description that includes neutrino flavor oscillations and, particle-anti-particle or chiral oscillations. In addition, our description is different from the usual neutrino oscillation theory that assumes neutrinos are relativistic. The relativistic assumption is often taken, because cosmological limits on the neutrinos absolute masses place them in the sub-eV range[18]; whereas, experiments are performed on neutrinos with energies in the keV, MeV, GeV, and recently the PeV ranges[19]. Non-relativistic neutrinos are predicted to exist in nature as the cosmic neutrino background ( $C\nu B$ ). Experiments to detect the  $C\nu B$  are under preparation (see for example, [20]), and we plan future studies of the  $C\nu B$  as an application of our description.

We consider the following situation when constructing our formulation. The neutrinos are produced by a weak interaction at  $t < 0$  and we treat them as part of a  $SU(2)_L$  doublet. The  $SU(2)_L$  doublet is used to assign a lepton family number of  $L_e, L_\mu$ , or  $L_\tau$  to the produced neutrino. We then formulate an operator for  $L$ . At time  $t = 0$ , we assign either a Dirac or Majorana mass to the neutrino. Then, the time evolution of the lepton family number operator becomes dependent on the mass and new features appear. We take the expectation value of the lepton family number operator and study the time evolution. For this Letter, we highlight information of the absolute mass hierarchy and type of mass can be seen for non-relativistic energies. We have previously discussed details of the formulation for the Majorana mass case[21], and we plan to provide more details for the Dirac mass case in a future work[22].

## DIRAC VS MAJORANA CALCULATION DIFFERENCES

### Dirac neutrino formulation

To begin with, we discuss the time evolution of the lepton family number for the Dirac neutrino case. The Lagrangian for the Dirac neutrinos  $\mathcal{L}^D$  is described as

$$\mathcal{L}^D = \overline{\nu_{L\alpha}} i \gamma^\mu \partial_\mu \nu_{L\alpha} + \overline{\nu_{R\alpha}} i \gamma^\mu \partial_\mu \nu_{R\alpha} - \theta(t) (\overline{\nu_{R\alpha}} m_{\alpha\beta} \nu_{L\beta} + \text{h.c.}), \quad (1)$$

for which we denote the neutrino flavors by the Greek subscripts,  $\nu_{L\alpha}$ . The first and second terms are kinetic ones and third term is Dirac mass one. The third term is controlled by

a step function. We define the lepton family number, for both the left- and right-handed Dirac neutrinos as

$$L_\alpha^L \equiv \int d^3x \overline{\nu_{L\alpha}} \gamma^0 \nu_{L\alpha}, \quad (2)$$

$$L_\alpha^R \equiv \int d^3x \overline{\nu_{R\alpha}} \gamma^0 \nu_{R\alpha}, \quad (3)$$

in which,

$$\nu_{L\beta} = V_{\beta j} \nu_{Lj}, \quad (4)$$

$$\nu_{R\alpha} = U_{\alpha i} \nu_{Ri}, \quad (5)$$

$$(U^\dagger)_{i\alpha} m_{\alpha\beta} V_{\beta j} = m_i \delta_{ij}. \quad (6)$$

We relate the two regions of Eq. (1) with the continuity condition at  $t = 0$ :

$$\nu_{Li}(t = 0_+) = \sum_{\alpha=e}^{\tau} V_{\beta i}^* \nu_{L\alpha}(t = 0_-) \quad (7)$$

$$\nu_{Ri}(t = 0_+) = \sum_{\alpha=e}^{\tau} U_{\beta i}^* \nu_{R\alpha}(t = 0_-). \quad (8)$$

Then, the time evolution of total lepton number for left-handed neutrinos is obtained as

$$\begin{aligned} \sum_{\alpha=e}^{\tau} L_\alpha^L(t) &= \sum_{i=1}^3 \sum_{\beta,\gamma} \int' \frac{d^3\mathbf{p}}{(2\pi)^3 2|\mathbf{p}|} \left\{ \left( \cos^2(E_i(\mathbf{p})t) + \frac{|\mathbf{p}|^2}{E_i(\mathbf{p})^2} \sin^2(E_i(\mathbf{p})t) \right) \right. \\ &\quad \times (V_{\beta i} V_{\gamma i}^* a_{L\beta}^\dagger(\mathbf{p}) a_{L\gamma}(\mathbf{p}) - V_{\beta i}^* V_{\gamma i} b_{L\beta}^\dagger(\mathbf{p}) b_{L\gamma}(\mathbf{p})) \\ &\quad \left. + \frac{m_i^2}{E_i(\mathbf{p})^2} \sin^2(E_i(\mathbf{p})t) (U_{\beta i} U_{\gamma i}^* b_{R\beta}(\mathbf{p}) b_{R\gamma}^\dagger(\mathbf{p}) - U_{\beta i}^* U_{\gamma i} a_{R\beta}(\mathbf{p}) a_{R\gamma}^\dagger(\mathbf{p})) \right\} \\ &+ \sum_{i=1}^3 \sum_{\beta,\gamma} \int_{p \in A} \frac{d^3\mathbf{p}}{(2\pi)^3 2|\mathbf{p}|} \left\{ \left( \frac{m_i}{E_i(\mathbf{p})} \cos(E_i(\mathbf{p})t) \sin(E_i(\mathbf{p})t) + \frac{i m_i |\mathbf{p}|}{E_i(\mathbf{p})^2} \sin^2(E_i(\mathbf{p})t) \right) \times \right. \\ &\quad \left. \left( -V_{\beta i} U_{\gamma i}^* (a_{L\beta}^\dagger(\mathbf{p}) b_{R\gamma}^\dagger(-\mathbf{p}) - a_{L\beta}^\dagger(-\mathbf{p}) b_{R\gamma}^\dagger(\mathbf{p})) + V_{\beta i}^* U_{\gamma i} (b_{L\beta}^\dagger(\mathbf{p}) a_{R\gamma}^\dagger(-\mathbf{p}) - b_{L\beta}^\dagger(-\mathbf{p}) a_{R\gamma}^\dagger(\mathbf{p})) \right) + \text{h.c.} \right\}, \quad (9) \end{aligned}$$

for which the integration region denoted by  $\int'$  does not include the zero momentum mode. Whereas, the integration region denoted by  $\int_{p \in A}$  is defined by writing the direction of the momentum  $\mathbf{n} = \frac{\mathbf{p}}{|\mathbf{p}|}$  in a spherical coordinate system of  $\theta$  and  $\phi$ . The region  $A$  corresponds to when the azimuthal angle  $\phi$  lies within the range  $[0, \pi)$  and the polar angle  $\theta$  within the range

$[0, \pi]$ . The right-handed counterpart of Eq.(9) is obtained by interchanging the matrices as  $U \rightarrow V$ ,  $V \rightarrow U$  and the handedness of the operators as  $a_{(L,R)} \rightarrow a_{(R,L)}$ ,  $b_{(L,R)} \rightarrow b_{(R,L)}$ . We prepare a left-handed neutrino flavor state given by

$$|\sigma_L(\mathbf{q})\rangle = \frac{a_{L\sigma}^\dagger(\mathbf{q})|0\rangle}{\sqrt{\langle 0|a_{L\sigma}(\mathbf{q})a_{L\sigma}^\dagger(\mathbf{q})|0\rangle}}, \quad (10)$$

which can take on the values of  $\sigma = (e, \mu, \tau)$ . We take the expectation value of the lepton family numbers of Eqs.(2) and (3) by sandwiching them with Eq.(10):

$$\begin{aligned} \langle \sigma_L(\mathbf{q})|L_\alpha^L(t)|\sigma_L(\mathbf{q})\rangle &= \sum_{i,j}^3 \left\{ \text{Re}(V_{\alpha i}^* V_{\sigma i} V_{\alpha j} V_{\sigma j}^*) \times \right. \\ &\quad \left( \cos(E_i(\mathbf{q})t) \cos(E_j(\mathbf{q})t) + \frac{\mathbf{q}^2}{E_i(\mathbf{q})E_j(\mathbf{q})} \sin(E_i(\mathbf{q})t) \sin(E_j(\mathbf{q})t) \right) \\ &\quad - \text{Im}(V_{\alpha i}^* V_{\sigma i} V_{\alpha j} V_{\sigma j}^*) \times \\ &\quad \left. \left( \frac{|\mathbf{q}|}{E_i(\mathbf{q})} \sin(E_i(\mathbf{q})t) \cos(E_j(\mathbf{q})t) - \frac{|\mathbf{q}|}{E_j(\mathbf{q})} \cos(E_i(\mathbf{q})t) \sin(E_j(\mathbf{q})t) \right) \right\}, \end{aligned} \quad (11)$$

$$\langle \sigma_L(\mathbf{q})|L_\alpha^R(t)|\sigma_L(\mathbf{q})\rangle = \sum_{i,j}^3 \left\{ \text{Re}(U_{\alpha j} V_{\sigma j}^* U_{\alpha i}^* V_{\sigma i}) \frac{m_i}{E_i(\mathbf{q})} \frac{m_j}{E_j(\mathbf{q})} \sin(E_i(\mathbf{q})t) \sin(E_j(\mathbf{q})t) \right\}. \quad (12)$$

### Majorana neutrino formulation

We discuss the multi-flavor case for Majorana neutrinos. This situation is written by the Lagrangian for Majorana neutrinos  $\mathcal{L}^M$ :

$$\mathcal{L}^M = \bar{\nu}_{\alpha L} i\gamma^\mu \partial_\mu \nu_{\alpha L} - \theta(t) \left( \frac{m_{\alpha\beta}}{2} \overline{(\nu_{\alpha L})^c} \nu_{\beta L} + \text{h.c.} \right), \quad (13)$$

in which the first term is kinetic one and the second term is the Majorana mass one. The second term is controlled by a step-function. In our previous paper [21], we obtained the expectation value of the lepton family number that is carried by the left-handed Majorana neutrinos as

$$\langle \sigma_L(\mathbf{p}) |L_\alpha^M(t)|\sigma_L(\mathbf{p})\rangle = \sum_{i,j}^3 \left\{ \text{Re}(V_{\alpha i}^* V_{\sigma i} V_{\alpha j} V_{\sigma j}^*) \times \right.$$

$$\begin{aligned}
& \left( \cos(E_i(\mathbf{q})t) \cos(E_j(\mathbf{q})t) + \frac{\mathbf{q}^2}{E_i(\mathbf{q})E_j(\mathbf{q})} \sin(E_i(\mathbf{q})t) \sin(E_j(\mathbf{q})t) \right) \\
& - \text{Im}(V_{\alpha i}^* V_{\sigma i} V_{\alpha j} V_{\sigma j}^*) \left( \frac{|\mathbf{q}|}{E_i(\mathbf{q})} \sin(E_i(\mathbf{q})t) \cos(E_j(\mathbf{q})t) - \frac{|\mathbf{q}|}{E_j(\mathbf{q})} \cos(E_i(\mathbf{q})t) \sin(E_j(\mathbf{q})t) \right) \Big\} \\
& - \sum_{i,j}^3 \left\{ \text{Re}(V_{\alpha i}^* V_{\sigma i}^* V_{\alpha j} V_{\sigma j}) \frac{m_i}{E_i(\mathbf{q})} \frac{m_j}{E_j(\mathbf{q})} \sin(E_i(\mathbf{q})t) \sin(E_j(\mathbf{q})t) \right\}, \quad (14)
\end{aligned}$$

in which the term  $\text{Re}(V_{\alpha i}^* V_{\sigma i}^* V_{\alpha j} V_{\sigma j})$  in the third line of Eq.(14) depends on the Majorana phases.

### Differences between the Dirac and Majorana formulations

We compare the three expectation value equations Eq.(11), Eq.(12) and Eq.(14) for the mass formulations. Firstly, the terms proportional to the MNS matrix of  $\text{Re}(V_{\alpha i}^* V_{\sigma i} V_{\alpha j} V_{\sigma j}^*)$  and  $\text{Im}(V_{\alpha i}^* V_{\sigma i} V_{\alpha j} V_{\sigma j}^*)$  are common between the formulations. Those terms are present in the left-handed Eq.(11) of the Dirac formulation and the first summation from Eq.(14) of the Majorana formulation. The differences between the formulations appear in the right-handed Eq.(12) of the Dirac formulation, in which the unitary matrix,  $U_{\alpha i}$ , related to the right-handed neutrinos appears with a positive overall sign. Whereas, in the Majorana formulation the term  $\text{Re}(V_{\alpha i}^* V_{\sigma i}^* V_{\alpha j} V_{\sigma j})$  is related to the Majorana phases appears with a negative overall sign. To help emphasize the effect of the sign differences we write the expectation value of the total lepton number for the Dirac formulation case

$$\sum_{\alpha} \langle \sigma_L(\mathbf{q}) | L_{\alpha}^L(t) | \sigma_L(\mathbf{q}) \rangle = 1 - \sum_i^3 |V_{\sigma i}|^2 \left( \frac{m_i}{E_i(\mathbf{q})} \right)^2 \sin^2(E_i(\mathbf{q})t), \quad (15)$$

for which inclusion of the right-handed summation over  $\alpha$  would cause Eq.(15) to be equal to one. On the other hand, the expectation value of the total lepton number for the Majorana neutrino case is obtained in our previous paper [21]:

$$\sum_{\alpha} \langle \sigma_L(\mathbf{q}) | L_{\alpha}^M(t) | \sigma_L(\mathbf{q}) \rangle = 1 - 2 \sum_i^3 |V_{\sigma i}|^2 \left( \frac{m_i}{E_i(\mathbf{q})} \right)^2 \sin^2(E_i(\mathbf{q})t). \quad (16)$$

### ILLUSTRATION OF NON-RELATIVISTIC DIFFERENCES

We plot here the left-handed expectation value of Eqs.(11),(12), and (14) to highlight the differences for non-relativistic region energies,  $|\mathbf{q}| \ll m_{lightest}$ . For the plots, we use

the best fit values of the PMNS mixing angles  $\theta_{12}, \theta_{23}$ , and  $\theta_{13}$ , the CP violating phase  $\delta_{\text{CP}}$ , and the mass squared differences  $\Delta m_{21}^2$  and  $\Delta m_{31}^2$  from the work of the NuFIT 5.0 (2020) collaboration[23]. Then, we are left to choose the absolute mass of the lightest neutrino  $m_1$  or  $m_3$ , the neutrino mass hierarchy, normal  $m_1 < m_2 \ll m_3$  or inverted  $m_3 \ll m_1 < m_2$ , the value of the momentum  $|\mathbf{q}|$ , the value of the time  $t$ , and the Majorana phases  $\alpha_{21}$  and  $\alpha_{31}$ . In this Letter, we always choose to have vanishing Majorana phases to emphasize the differences between the Dirac and Majorana mass formulations. The details on the effects of the Majorana phases, in the Majorana formulation, is found in our previous work[21].

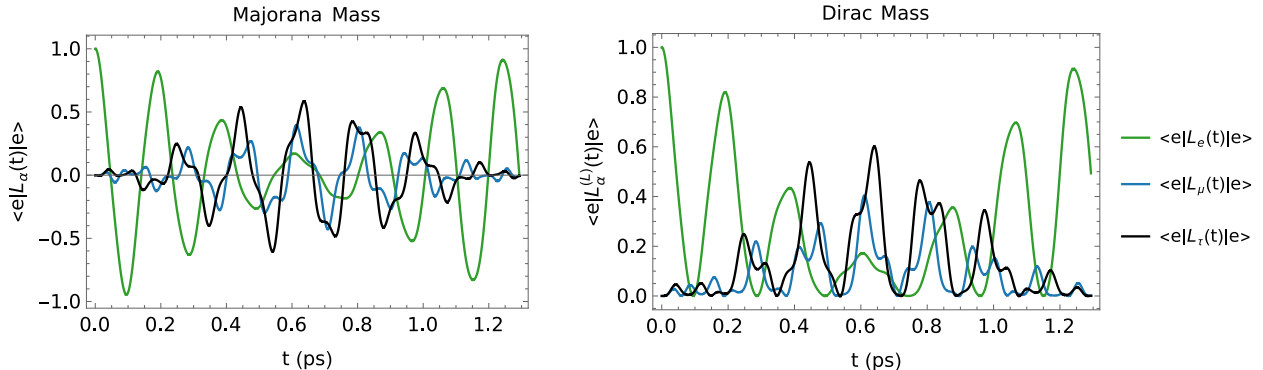


FIG. 1. Comparison of the mass term formulations for a normal mass hierarchy. In both panels the value of the momentum is  $|\mathbf{q}| = 0.0002$  eV and the lightest neutrino mass is 0.01 eV, which means all the neutrinos are non-relativistic. The left panel is the complete Majorana formulation, when both of the Majorana phases are set to zero. The right panel is only the left-handed Dirac formulation. Notice that the vertical axis is not equally scaled between the two panels.

To begin with, we illustrate the effects of the mass dependent terms from Eqs.(12) and 14 in Fig.1. In the left panel of Fig. 1, the expectation values are constrained between  $-1$  and  $1$ . This constraint is found in Eq.(16). We interpret the sign change as particle-anti-particle oscillations that are from the lepton number violating nature of the Majorana mass. A comparison to the right panel shows the expectation values of the Dirac mass formulation are constrained between  $0$  and  $1$ . We only plot the left-handed chiral operator; however, the right-handed operator features the same constraint. The difference in the lower bound of the constraints, Majorana being  $-1$  and Dirac being  $0$ , is because of the sign of the mass dependent term in the expectation values. Specifically, the sign of Majorana mass

dependent term is negative; whereas, the sign of the Dirac mass dependent term is positive. As this bound is mass dependent, differences between the Majorana and Dirac formulations are suppressed when  $|\mathbf{q}| \gg m_i$ .

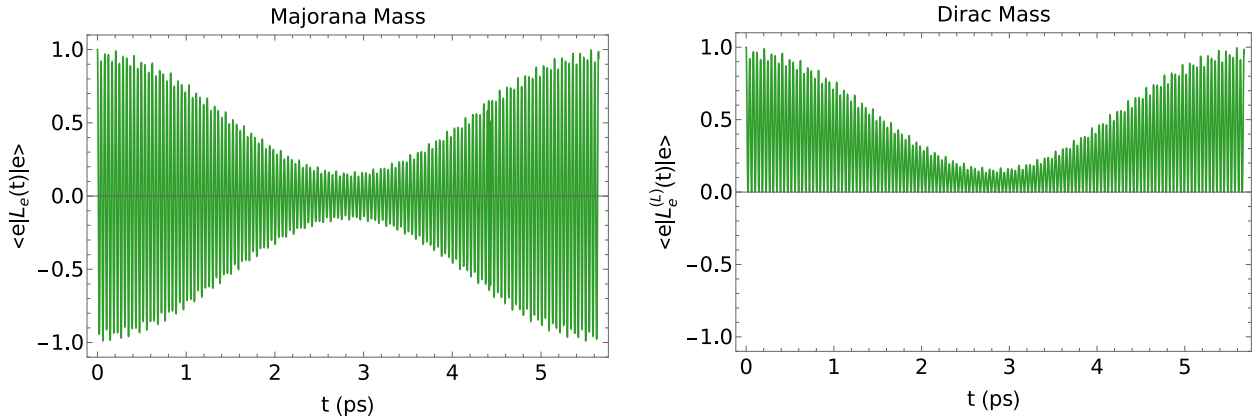


FIG. 2. The time evolution of the expectation value is taken for only the electron neutrino operator with an inverted mass hierarchy. The same values for the momentum and lightest neutrinos mass are used as in Fig.1. The left panel is the Majorana mass formulation and both of the Majorana phases are set to zero. The right panel is the left-handed Dirac mass formulation.

Next, we illustrate the effects of the mass hierarchy. In Fig.2, we only plot the electron family number  $L_e$ ; however, the effects that are discussed in this paragraph are the same for the muon and tauon family numbers. The left(right) panel of Fig.2 shows the inverted mass hierarchy case for the Majorana(Dirac) formulation. We compare those with the normal mass hierarchy cases of Fig.1. The differences of the hierarchies is seen in the period of oscillations of the expectation value. These differences are due to a combination of two effects that occur in the non-relativistic region. First, there are two types of periods in our formulation, those that are dependent on the addition of energies  $E_i + E_j$  and those that are dependent on the difference of energies  $E_i - E_j$ . When the neutrinos are non-relativistic, the  $E_i - E_j$  periods are similar to the mass differences; whereas, the  $E_i + E_j$  periods are more representative of the absolute masses. Second, the momentum dependent terms of Eqs.(11) and (14) are suppressed. That suppression leads to larger amplitudes for the periods of  $E_i + E_j$  and smaller amplitudes for the periods of  $E_i - E_j$ . The combination of those two effects lead the  $E_i + E_j$  periods, which are representative of the absolute masses, to become enhanced in the non-relativistic region.

Lastly, we illustrate the momentum dependence of the expectation values in Fig.3 and

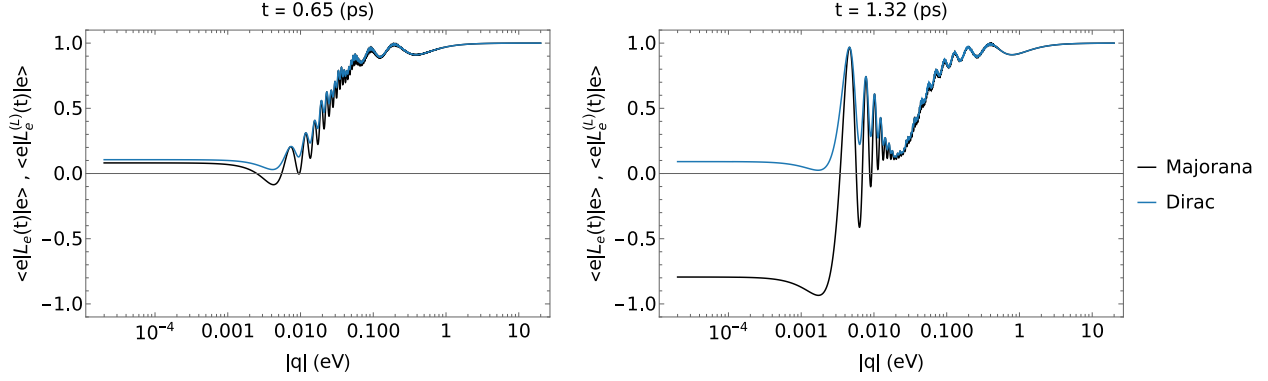


FIG. 3. The momentum variation of the expectation value for the electron neutrino operator at fixed time slices  $t$ . In both panels, the normal mass hierarchy is taken and the value of the lightest neutrino mass is 0.01 eV. The values of  $t = 0.65$  ps and  $t = 1.32$  ps are chosen to emphasize the changes to the steady state value in small momentum region. Both of the Majorana phases are set to zero.

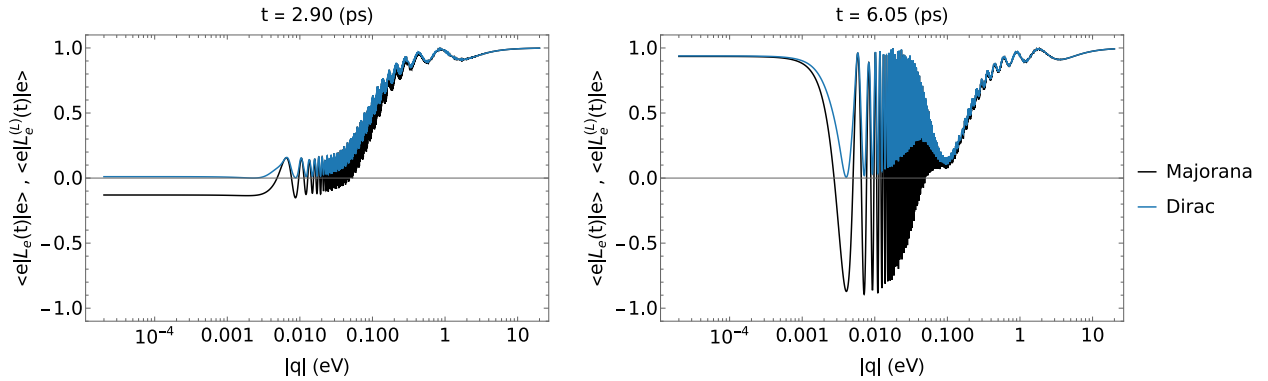


FIG. 4. The momentum variation of the expectation value for the electron neutrino operator at fixed time slices  $t$ . In both panels, the inverted mass hierarchy is taken and the lightest neutrino mass is 0.01 eV. The values of  $t = 2.90$  ps and  $t = 6.05$  ps are chosen to emphasize the changes to the steady state value in small momentum region. Both of the Majorana phases are set to zero.

Fig.4. Similar to Fig.2, we only plot the electron family number. The panels of Fig.3 are for the normal hierarchy case. In both panels the expectation values of the Majorana and Dirac formulations are plotted. The difference between the panels is the time slice we chose. We chose the times  $t = 0.65$  ps ( $1.32$  ps) based on the min(max) amplitude of the electron family envelope in Fig.1. From comparing the two time slices, the Majorana formulation can take on positive and negative values; whereas, the Dirac formulation is always positive. In the

right panel of  $t = 1.32$  ps the Majorana formulation reaches a negative steady-state value when the momentum is smaller than the mass  $|\mathbf{q}| \ll m_i$ . When the momentum and mass are of similar values  $|\mathbf{q}| \sim m_i$  the expectation value oscillates for which the period and amplitude of the oscillation depends on the chosen time slice. For momentum's larger than the masses  $|\mathbf{q}| \gg m_i$ , the expectation value reaches the same steady state value in both panels. We plot the inverted hierarchy case in Fig.4, which has the same features of Fig.3. We highlight the change of hierarchy has two identifying results. First, the time slice of  $t = 2.90$  ps (6.05 ps) are based on the min(max) amplitudes of the envelope in Fig.2. Second, the oscillations in the region of  $|\mathbf{q}| \sim m_i$  have decreased in period. This decrease in period is similar to the comparison made between Fig.1 and Fig.2. The oscillation and settling effect could be an interesting tool for studying the absolute mass range of the neutrinos, as this effect occurs for any time value.

## CONCLUSION

We have proposed a novel formulation for neutrino oscillations from a QFT point of view. This formulation can be applied to both relativistic and non-relativistic energies for neutrinos. To achieve that, we treated the neutrinos from the weak interaction to have either Dirac or Majorana mass. Then, we considered the neutrinos to have been produced with a specific lepton family number associated with the neutrino's flavor. From the connection between the specific lepton family number and the neutrino's mass, we constructed a lepton number operator for the massive neutrinos. By taking the expectation value of the lepton number operator, the flavor oscillations were studied in the relativistic and the non-relativistic energy regions. We have shown that, in the non-relativistic region, the absolute mass hierarchy and the type of neutrino mass are distinguished. Thus, future studies of non-relativistic region could be used as an additional approach to test the absolute mass hierarchy and the type of neutrino mass.

The work of T.M. is supported by Japan Society for the Promotion of Science (JSPS) KAKENHI Grant Number JP17K05418. We would like to thank Uma Sankar and Koichi Hamaguchi for useful comments and suggestions during the initial presentations of this work.

- 
- \* apri014@lipi.go.id  
† d195016@hiroshima-u.ac.jp  
‡ yuta-kawamura@hiroshima-u.ac.jp  
§ ya-matsuo@hiroshima-u.ac.jp  
¶ morozumi@hiroshima-u.ac.jp  
\*\* yu-shimizu@hiroshima-u.ac.jp  
†† zhizailitian7@gmail.com
- [1] J. N. Bahcall, AAPPS Bull. **12**, no.4, 12-19 (2002)  
[2] K. Abe *et al.* (Super-Kamiokande), Phys. Rev. D **83**, 052010 (2011)  
[3] B. Aharmim *et al.* (SNO), Phys. Rev. C **81**, 055504 (2010)  
[4] B. Pontecorvo, Sov. Phys. JETP **7**, 172 (1958) [Zh. Eksp. Teor. Fiz. **34**, 247 (1957)].  
[5] Z. Maki, M. Nakagawa and S. Sakata, Prog. Theor. Phys. **28**, 870 (1962).  
[6] B. Abi *et al.* (DUNE), Eur. Phys. J. C **80**, no.10, 978 (2020)  
[7] K. Abe *et al.* (Hyper-Kamiokande Proto-), PTEP **2015**, 053C02 (2015)  
[8] K. Abe *et al.* (Hyper-Kamiokande), PTEP **2018**, no.6, 063C01 (2018)  
[9] E. Baussan *et al.* (ESSnuSB), Nucl. Phys. B **885**, 127-149 (2014)  
[10] S. Ahmed *et al.* (ICAL), Pramana **88**, no.5, 79 (2017)  
[11] F. An *et al.* (JUNO), J. Phys. G **43**, no.3, 030401 (2016)  
[12] M. Aker *et al.* (KATRIN), Eur. Phys. J. C **80**, no.3, 264 (2020)  
[13] M. J. Dolinski, A. W. P. Poon and W. Rodejohann, Ann. Rev. Nucl. Part. Sci. **69**, 219-251 (2019)  
[14] W. H. Furry, Phys. Rev. **56**, 1184-1193 (1939)  
[15] J. N. Bahcall and H. Primakoff, Phys. Rev. D **18**, 3463-3466 (1978)  
[16] J. Schechter and J. W. F. Valle, Phys. Rev. D **23**, 1666 (1981)  
[17] Z. z. Xing, Phys. Rev. D **87**, no.5, 053019 (2013)  
[18] N. Aghanim *et al.* (Planck), Astron. Astrophys. **641**, A6 (2020)  
[19] J. A. Formaggio and G. P. Zeller, Rev. Mod. Phys. **84**, 1307-1341 (2012)  
[20] M. G. Betti *et al.* (PTOLEMY), JCAP **07**, 047 (2019)

- [21] A. S. Adam, N. J. Benoit, Y. Kawamura, Y. Matsuo, T. Morozumi, Y. Shimizu, Y. Tokunaga and N. Toyota, PTEP **2021**, (2021) doi:10.1093/ptep/ptab025
- [22] In preparation.
- [23] I. Esteban, M. C. Gonzalez-Garcia, M. Maltoni, T. Schwetz and A. Zhou ([www.nu-fit.org](http://www.nu-fit.org)), JHEP **09**, 178 (2020)